Effect of Salt on the Excited-State Dynamics of Malachite Green in Bulk Aqueous Solutions and at Air/Water Interfaces: a Femtosecond Transient Absorption and Surface Second Harmonic Generation Study†

Angela Punzi, Gaëlle Martin-Gassin, Jakob Grilj, and Eric Vauthey*

Department of Physical Chemistry, University of Geneva, 30 Quai Ernest-Ansermet, 1211, Genève 4, Switzerland

Received: February 28, 2009; Revised Manuscript Received: April 17, 2009

The ultrafast excited-state dynamics of Malachite Green (MG) in bulk aqueous solutions and at air/water interfaces, in particular the effect of the presence of various sodium salts in the aqueous phase, has been investigated by transient absorption and surface second harmonic generation. In bulk solutions, a slowing down of the ground-state recovery that can be unambiguously ascribed to the formation of aggregates of various sizes is observed at high (>0.3 M) salt concentrations only, with the exception of NaSCN where an effect is already found at 0.05 M. At the interface, small amounts of salt result in two effects: 1) an increase of the stationary surface second harmonic signal and 2) a slowing down of the ground-state recovery of MG. These phenomena are explained by the formation of aggregates due to an increase of the interfacial MG concentration upon addition of salt. The dependencies of both effects on salt concentration are correlated and vary with the anion as $SCN^- > Br^- > SO_4^- > Cl^-$. This order is almost the opposite as that in the Hofmeister series for the salting-out strength.

Introduction

Over the past decades, liquid interfaces (air/liquid and liquid/liquid) have attracted considerable attention in different fields of science, where they play a crucial role.[1] The bulk liquid phase, where molecules are randomly oriented, can be characterized by isotropic properties such as viscosity or dielectric constant. The situation is totally different at liquid interfaces, where the asymmetry of forces leads to an anisotropy of molecular orientation and hence to totally different properties. However, the measurement of these new features remains a major problem, and therefore, despite the numerous studies on liquid interfaces, our current knowledge is still relatively small. A major difficulty for experimentalists is to discriminate the interfacial region from the bulk phase, because, in conventional optical spectroscopies, the response from the interface, which consists of a few molecular layers, is totally buried in that originating from the bulk. There are essentially two approaches to circumvent this problem. The first is to confine the optical probe beam near the interface. This is in general done by using the evanescent optical field generated by total internal reflection (TIR) for probing the interfacial region. Such evanescent waves have been used to excite fluorescence,[2,3] for probing absorbance,[4] and for generating or probing transient gratings in four wave-mixing experiments.[5,6] However, this approach based on TIR cannot be used for investigating air/liquid interfaces. Confinement of the probe light by using the near field at the output of a microscope tip to explore the interface has also been demonstrated.[7,8]

The other common approach is based on the measurements of even order, second or fourth, nonlinear response which is, within the dipolar approximation, zero in the bulk and thus arises from the interfacial region only. Surface second-harmonic generation (SSHG),[9,10] and sum-frequency generation (SSFG)[11] are the most frequently used techniques, although fourth order nonlinear methods have also been implemented.[12,13]

Both SSHG and SSFG have been mostly used to probe stationary properties, the signals being monitored as a function of (1) the probe frequency to record either a vibrational spectrum of the interfacial region,[14−17] or an electronic absorption spectrum of an adsorbate at the interface, (2) the polarization of the probe and/or signal field to obtain information on the orientation of molecules adsorbed at the interface,[18,19] or (3) a parameter such as pH, salt concentration, or temperature to investigate specific interfacial properties.[20]

On the other hand, applications of transient SSHG (TSSHG) and SSFG to obtain direct dynamic information are much more scarce. This field has been pioneered by Eisenthal and his group, who have investigated the dynamics of various photoinduced processes at liquid interfaces.[9,21−23]

TSSHG is usually performed at a single wavelength and therefore the interpretation of the measured time profiles might by ambiguous, especially when working in the femto- and picosecond time scales where many phenomena, such as solvent and vibrational relaxation, take place additionally to population dynamics. In principle, all these processes can be disentangled in the bulk by performing transient absorption (TA) measurements with a white-light continuum. Although this combination of TA with white light and TSSHG spectroscopy is particularly powerful for evidencing the difference between bulk and interfacial dynamics, it has not been really used until now.

We present here our detailed investigation of the excited-state dynamics of Malachite Green (MG, Chart 1) at air/water interfaces using TSSHG and in bulk aqueous solutions using TA. This dye is known to have a very short lifetime of its S_1 state resulting from a very efficient nonradiative deactivation associated with the large amplitude motion of the phenyl substituents.[24] Because of the friction dependence of its S_1 lifetime, MG can be used as local viscosity probe. TSSHG

† Part of the "Hiroshi Masuhara Festschrift".

* Corresponding author. E-mail: eric.vauthey@unige.ch.

10.1021/jp9018662 CCC: $40.75
Published on Web 05/08/2009

CHART 1: Malachite Green Oxalate

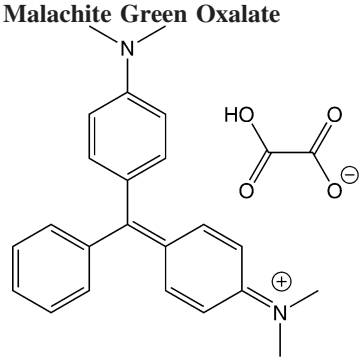

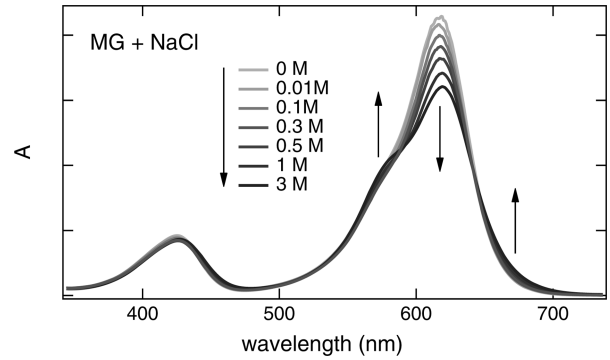

Figure 1. Steady-state absorption spectra of MG in water with various NaCl concentrations.

measurements of MG at air/liquid, liquid/liquid, and air/solid interfaces have already been reported.[25−27] At liquid interfaces, a substantial slowing down of the excited-state relaxation was found relative to the bulk phase, indicative of higher friction.[25] Here, we have particularly focused our attention on the effect of the addition of sodium salts in the aqueous phase on both the bulk and the interfacial dynamics of MG excited state. We show that addition of salt has a profound impact on the interfacial dynamics and that the strength of this effect depends substantially on the nature of the anion.

Experimental Section

Samples. Malachite Green oxalate (MG), NaCl, and NaSCN were purchased from Fluka, whereas Na_2SO_4 and NaBr were from Merck. All compounds were used without further purification. Unless specified, the dye concentration in deionized water amounted to 1.5×10^{-4} M for both bulk and interfacial studies. The pH of the MG solutions with and without salt was around 3.5. Under these conditions, the monocation is the dominant form of MG.[24] No significant degradation of the samples was observed after the measurements.

Transient Absorption (TA) Measurements. The femtosecond TA setup has already been described in detail elsewhere.[28] Briefly, TA measurements were performed by using two different pump wavelengths, 615 and 400 nm. Excitation at 615 nm was achieved with the tunable output of a home-built noncollinear optical parametric amplifier (NOPA) fed by the 800 nm output of a standard 1kHz amplified Ti:Sapphire system (Spectra-Physics). The duration of the pulses was around 50 fs and their energy on the sample about 2 μJ. Excitation at 400 nm was performed by frequency-doubling part of the output of the amplified Ti:sapphire system. The duration and energy of these 400 nm pulses were about 100 fs and 2 μJ, respectively. Transient spectra were obtained by probing with a white-light continuum, generated by focusing 800 nm pulses into a 3 mm-thick CaF_2 plate. The polarization of the probe pulses was at magic angle relative to that of the pump pulses. After acquisition, all spectra were corrected for the chirp of the white-light probe pulses. The full width at half-maximum of the instrument response function was around 200 fs. The sample solutions were circulated through a 0.2 mm-thick quartz flow-cell connected to a peristaltic pump. The sample solutions were kept at a constant temperature of 10 °C as for the air/water interface measurements.

Transient Surface Second Harmonic Generation (TSSHG). The experimental arrangement for femtosecond TSSHG was based on the same amplified Ti:Sapphire system as described above. The pump pulses at 615 nm, with an energy of 6 μJ and a duration of about 50 fs, were generated with a commercial NOPA (Clark-MXR). These pulses were sent through a quarter waveplate to achieve circular polarization and were then focused perpendicularly onto the interface to a spot of about 1.5 mm diameter. Probing was performed using 800 nm pulses with 5 μJ energy, 100 fs duration, and s-polarization. The angle of incidence of these pulses on the interface was set at 70°, and their spot size had about 1 mm diameter. Just before the sample, the probe pulses passed a 450 nm cutoff filter to eliminate possible second harmonic signal arising from the surfaces of the various optical elements. The sample was located in a 3 mm-deep cylindrical Teflon dish of 35 mm diameter, which was rotated at 1 turn/s. Evaporation of the sample solution was minimized by using a constant temperature of 10 °C. The reflected probe beam containing the SSHG signal at 400 nm was passed through two BG23 cutoff filters to eliminate the 800 nm light and then focused onto the entrance slit of a 0.25 m monochromator (Oriel Cornerstone) equipped with a photomultiplier tube (Hamamatsu, C8728). The output signal was then amplified and processed by a gated integrator and boxcar averager module (Stanford Research Systems, SR250) and a computer interface (SR245). The monochromator, the SR245 module, as well as the translation stage for the pump−probe delay (PI M-531DG) were controlled by a computer program operating under LabVIEW (National Instruments).

Results and Discussion

MG in Bulk Aqueous Solutions. Figure 1 shows the absorption spectrum of MG in water with increasing NaCl concentration. The bands centered at 617 and 424 nm can be ascribed to the S_0-S_1 and S_0-S_2 transitions, respectively.[24] Upon addition of NaCl, the 424 nm band remains essentially the same, whereas substantial changes of the 617 nm band can be observed. Indeed, the intensity at the band maximum decreases, and a shoulder at about 580 nm as well as a broadening of the red edge of the band appear. These features can be ascribed to the aggregation of MG molecules,[29] the blue shoulder and the broadened red edge being due to excitonic splitting. The apparent much higher intensity of the blue excitonic band compared to the red one suggests a H-type aggregate where the MG molecules are arranged in a face-to-face conformation with the transition dipole moments in parallel.[30]

A similar effect was observed upon addition of the same amounts of Na_2SO_4 and NaBr. In contrast, NaSCN was found to strongly favor aggregations and even precipitation already at very low concentrations (0.01−0.05 M) (Figure S1 in the Supporting Information). Thus, TA and TSSHG investigations with this salt were carried out after filtering out the precipitate.

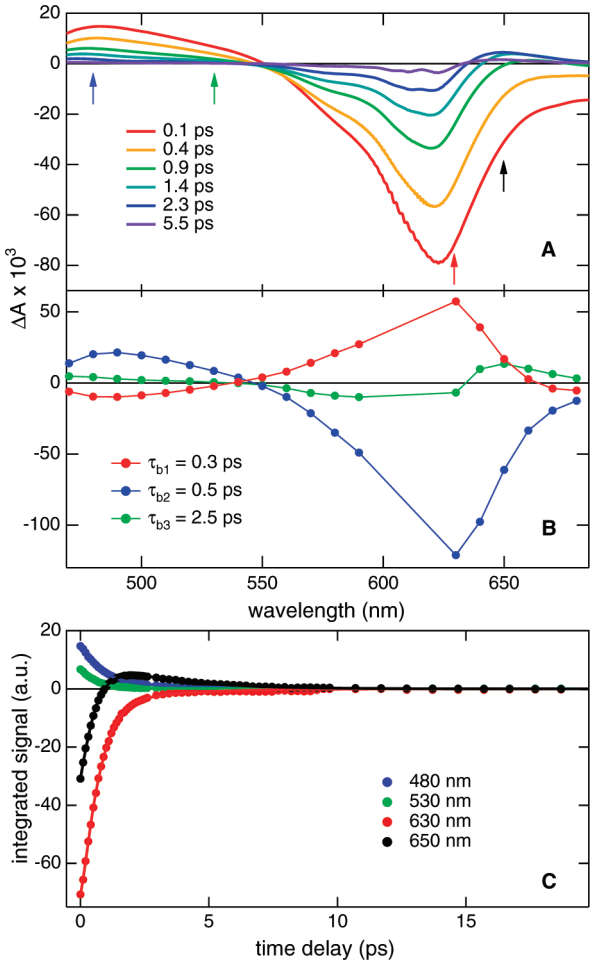

Figure 2. (A) TA spectra measured with MG in water at different time delays after 615 nm excitation; (B) decay-associated spectra obtained from global analysis; and (C) time profiles of the TA intensity integrated over 2 nm at different wavelengths (arrows in A) with the best fits obtained by global analysis (solid lines).

Figure 2A shows TA spectra measured with an aqueous MG solution at different time delays after excitation at 615 nm. At early time, these spectra consist of a positive band below 550 nm that can be ascribed to excited-state absorption and in a negative band at longer wavelength that arises mainly from the bleach of the S_0-S_1 absorption and from stimulated emission. As time goes on, the intensity of both positive and negative bands decreases and a new positive band appears around 650 nm. Finally, all these features decay to zero within about 8−10 ps. Figure 2C shows time-profiles of the TA intensity integrated over 2 nm at four different wavelengths. Global analysis of such profiles throughout the whole spectral window was performed using a sum of exponential functions. Not less than three exponentials had to be used to reproduce all time profiles. The resulting global time constants are listed in Table 1, whereas the associated spectra are depicted in Figure 2B.

These TA spectra are fully consistent with previous ultrafast investigations of MG in water and are discussed in terms of the energy level scheme depicted in Figure 3.[31−37] Excitation of MG in the S_0-S_1 transition is followed by ultrafast relaxation from the Franck−Condon S_1 state to equilibrium. According to the literature, this process is slightly solvent dependent and involves torsional re-equilibration of the excited state.[33,35] The shortest time constant found here, τ_{b1}, can be associated with this relaxation step. This process is followed by a nonradiative transition to an intermediate state S_x. The absorption spectrum

TABLE 1: Time Constants Obtained from the Global Analysis of the TA Spectra of MG in Bulk Aqueous Solutions (Limit of Error: ± 5%)

salt	λ_p (nm)[a]	τ_{b1} (ps)	τ_{b2} (ps)	τ_{b3} (ps)	τ_{b4} (ps)
none	615	0.3	0.5	2.5	
none[b]	400	0.4	0.5	2.8	
NaCl, 3M	400	0.3	0.7	3.2	50
NaSCN, 0.05 M	400	1.6	2.1	8.8	120

[a] Pump wavelength. [b] Same results with 0.05 to 0.3 M NaCl, NaBr and Na_2SO_4.

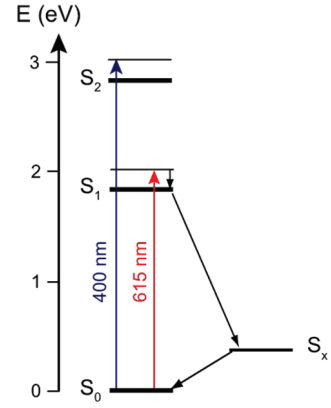

Figure 3. Energy-level scheme pertaining to the excited-state dynamics of MG.

of S_x differs slightly from that of the thermally equilibrated S_0 state and its population is responsible for the positive TA band around 650 nm. This S_x state has been interpreted as a vibrationally hot ground state by some authors,[34] and as a twisted ground state by others.[32] Independent of its exact nature, which in both cases corresponds to a nonrelaxed ground-state, its population can be associated with the second time constant, τ_{b2}, whereas its decay can be related to the longest time constant, τ_{b3}. Consequently, the amplitude spectrum associated with τ_{b3} can be ascribed to the TA spectrum of the S_x population, whereas that associated with τ_{b2} should be dominated by the TA spectrum of the S_1 state, with the bleach of the S_0-S_1 absorption, the stimulated emission and the excited-state absorption. Finally, the spectrum associated with τ_{b1} supports the assignment of this time constant to the equilibration of the S_1 population, as it is essentially mirror image of the TA spectrum of the S_1 state, indicating that τ_{b1} corresponds to the build up of this population. It should be noted that the time constants obtained from a multiexponential global fit cannot be directly identified with the lifetimes of the species involved the scheme shown in Figure 3. However, these time constants can be considered as reasonable estimates. More rigorous analysis requires global fit with target analysis using a function accounting for the kinetics of all the species. Whereas this can be done for MG in pure water, this is much more problematic in the presence of salt as the number of species present is not known. Therefore, multiexponential fit, allowing direct comparison of the dynamics with and without salt, has been preferred here.

TA spectra of MG in pure water have also been recorded upon 400 nm excitation. They were almost the same as those measured upon 615 pumping, the main difference being the slightly larger amplitude of the positive 650 nm band. Global analysis using a triexponential function yielded similar time constants (Table 1) and associated amplitude spectra. This pump wavelength results in the population of the S_2 state (Figure 3), which has been shown to have a 270 fs lifetime.[38] The similitude

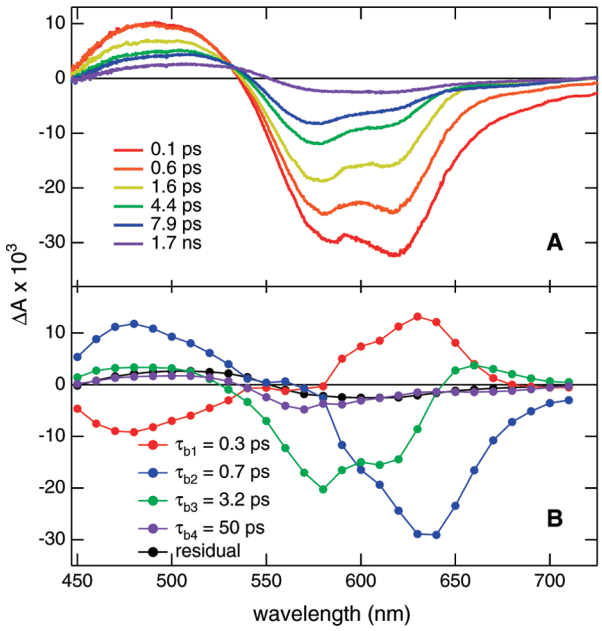

Figure 4. (A) TA spectra measured at different time delays after 400 nm excitation of MG in water with 3 M NaCl and (B) decay-associated spectra obtained from the global analysis.

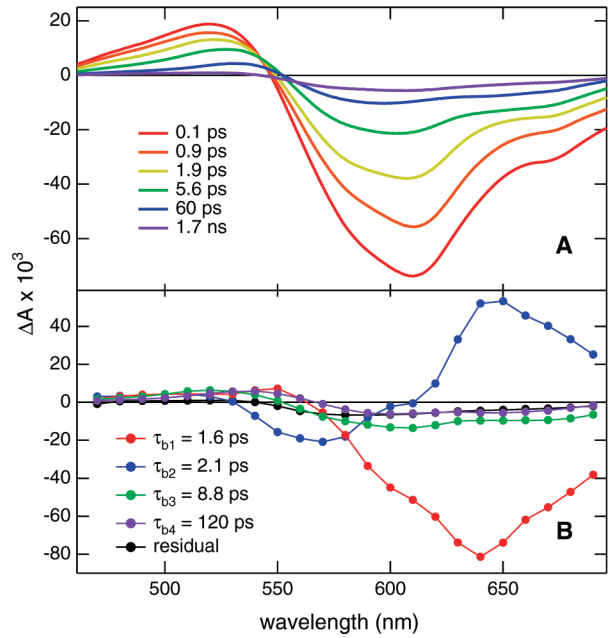

Figure 5. (A) TA spectra measured at different time delays after 400 nm excitation of MG in water after addition of 0.05 M NaSCN and (B) decay-associated spectra obtained from the global analysis.

of the τ_{b1}-associated spectra measured with both pump wavelengths indicates that the S_2 state of MG does not absorb significantly in the spectral window investigated here. Population of the S_x state probably takes place in parallel to the relaxation toward the equilibrium S_1 state.

The higher amplitude of the 650 nm TA band upon 400 nm excitation is consistent with the S_x state being a vibrationally hot ground state, the nonradiative deactivation from S_2 involving the dissipation of much more energy.

TA spectra recorded upon 400 nm excitation of aqueous MG solutions after addition of 3 M NaCl are shown in Figure 4A. They consist of a positive TA bands below about 550 nm and in a negative one at longer wavelength. The positive TA band at 650 nm observed without salt is not visible here. At early time delays, the negative band exhibits maxima at 585 and 620 nm. As time goes on, the relative intensity of these two maxima changes substantially and, after about 3 ps, the 620 nm feature is reduced to a shoulder. The decrease in the amplitude of this negative band is accompanied by a parallel blue shift of the maximum from 585 to about 575 nm. On the other hand, the positive band centered at about 490 nm decreases continuously without significant change of shape. Global analysis of the TA time profiles recorded over the whole spectral window required not less than four exponential functions additionally to a constant residual, with the time constants listed in Table 1 and the associated amplitude spectra shown in Figure 4B.

The amplitude spectra associated with τ_{b1} and τ_{b2} are essentially the same as those found without NaCl. On the other hand, the spectrum associated with τ_{b3} consists of a negative band centered at about 590 nm and two positive bands, one below 550 nm and the other at about 650 nm. The position of the negative band corresponds well with the shoulder assigned to the high frequency excitonic transition of MG aggregates (Figure 1). These spectra suggest the coexistence of MG in various forms of aggregation. The two shortest time constants most probably arise from nonaggregated MG because they are essentially identical to those measured without salt and are associated with similar amplitude spectra. The next time constant, τ_{b3}, most probably accounts for two processes occurring on a similar time scale: (1) the decay of the S_x state population of nonaggregated MG, hence the presence of the 650 nm band in the associated spectrum, and (2) the ground-state recovery of aggregated MG. The longer excited-state lifetime of these aggregates compared to the monomeric form of MG can be accounted for by the reduced mobility of the phenyl groups. The spectra associated with τ_{b4} and with the residual intensity are quite like that related to τ_{b3}, except that the 650 nm band due to the S_x state population is lacking. Consequently, these slower decaying components can be ascribed to larger aggregates.[26,39] Nonradiative deactivation of these excited aggregates does most probably not take place via large amplitude motion, as the latter is probably strongly inhibited. However, the exact channel cannot be inferred for the present data. The TA spectra and the associated dynamics recorded with NaCl concentrations in the 0.05−0.3 M range were essentially identical to those measured without NaCl.

The TA spectra recorded upon addition of 0.05 M NaSCN differ from those measured with NaCl, as illustrated in Figure 5A. In this case, the negative band exhibits a shoulder on its red side, at about 670 nm. Here again, four exponential functions were required in the global analysis (Table 1 and Figure 5B). Contrary to pure water and to NaCl solutions, the excited-state dynamics does not exhibit any subpicosecond component. The two shortest time constants, τ_{b1} and τ_{b2}, are very similar, around 2 ps, and their associated amplitude spectra are almost mirror image. Therefore, the error on these amplitudes should be quite large. The spectrum associated with τ_{b1} is dominated by a negative band that is broader than that of the MG monomer. This time constant most probably corresponds to the relaxation of excited MG monomers and/or of small MG aggregates. The spectra associated with τ_{b3}, τ_{b4}, and the residual intensity, are all very similar to those found with NaCl and ascribed to larger aggregates. On the other hand, the origin of τ_{b2} is relatively unclear. The presence of a positive band at 650 nm suggests that this time constant involves the relaxation of the S_x state population, however other processes occurring on this time scale could also be

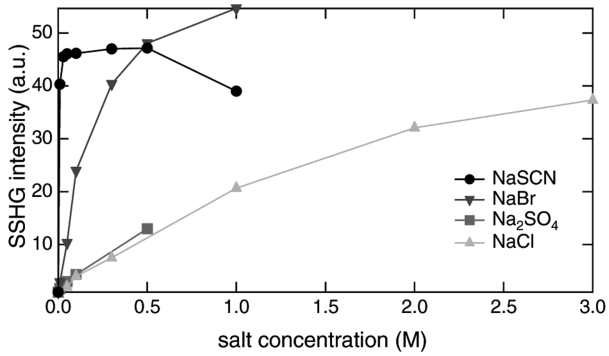

Figure 6. Effect of salt concentration on the stationary SSHG intensity measured with MG at the air/water interface.

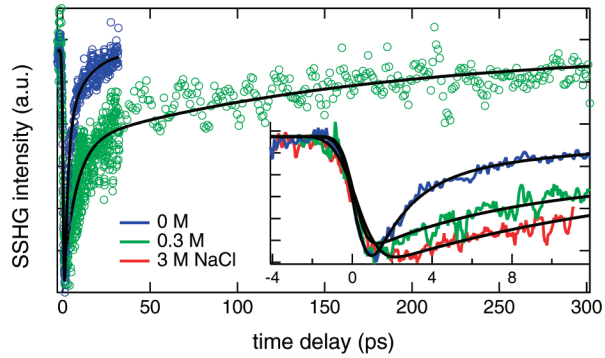

Figure 7. Intensity-normalized TSSHG profiles recorded at 400 nm after 615 nm excitation of MG at air/water interfaces with various NaCl concentrations and best biexponential fits (inset: early dynamics).

implicated. The presence of a relatively large number of different species upon addition of NaSCN is supported by the absence of an isosbestic point that can be observed in the TA spectra without salt (Figure 2A) and with NaCl (Figure 4A). Although in the latter case an isosbestic point is not really expected, its existence suggests that aggregates with rather similar spectra and dynamic properties are formed.

Finally, it should be noted that the addition of NaBr and Na_2SO_4 in the 0.05−0.3 M concentration range did not affect the TA spectra and the associated dynamics.

MG at Air/Water Interfaces. Figure 6 shows the concentration dependence of added salts on the stationary SSHG signal from MG at air/water interface. A strong signal enhancement is observed with all salts investigated. This increase is not due to the nonlinear response of the added salt because the SSHG intensity recorded under the same experimental conditions but without MG is negligibly small. The strongest concentration dependence is observed with NaSCN, with which the signal intensity increases by a factor of 40 at 10 mM. Saturation of this effect starts above about 30 mM NaSCN and at 1 M, the precipitation of MG leads to a decrease of the signal intensity. An even stronger signal enhancement, more than a factor 50, is found with NaBr, but at a larger concentration. Finally, the weakest effect is found with Na_2SO_4 and NaCl, both of which exhibiting a similar concentration dependence. As discussed in more detail later, this enhancement of the signal can be ascribed to the different salting-out efficiencies.[40−43]

Figure 7 shows TSSHG signals recorded upon 615 nm excitation of MG solutions containing various NaCl concentrations. Excitation of MG at 615 nm results in a substantial depletion of the SSHG signal, typically 14−16% of the total SSHG intensity, that can be explained by the bleach of the S_0-S_2 absorption and thus by a decrease of the resonant enhancement of the signal at 400 nm. Therefore, the recovery of the SSHG signal intensity reflects the repopulation of the ground state.

TABLE 2: Time Constants and Relative Amplitudes Obtained from the Best Fit of a Biexponential Function to the Square Root of the TSSHG Profiles Recorded at Air/Water Interfaces with Various Salt Concentrations (Limits of Error on τ_{i1}: ± 5%, on τ_{i2}: ± 10%, See Text)

salt	concentration (M)	τ_{i1} (ps)	A_{i1}	τ_{i2} (ps)	A_{i2}
none		1.1	0.85	8.3	0.15
NaCl	0.05	1.4	0.82	60	0.18
	0.3	6.8	0.60	∼150	0.40
	1	9.4	0.59	∼400	0.41
	3	12.8	0.62	∼200	0.38
NaSCN	0.05	10.3	0.75	∼200	0.25
	0.3	13.3	0.48	∼500	0.52
	1	13.5	0.50	∼500	0.50
Na_2SO_4	0.05	1.9	0.79	11	0.21
	0.1	3.9	0.55	∼100	0.45
	0.3	4.2	0.48	∼150	0.52
	0.5	4.5	0.53	∼200	0.47

As the SSHG intensity is proportional to the square of the population, whereas the TA intensity is linearly related to the population, the profiles of the square root of the TSSHG signal have been used for the multiexponential fit. The square root of the TSSHG signal with MG in pure water can be reproduced using a biexponential function with 1.1 and 8.3 ps time constants (Table 2). The 1.1 ps time constant is in reasonable agreement with that of 2.0 ± 0.3 ps reported by Shi et al. for the same system.[25] The fact that the profiles were analyzed here by taking the response function of the experiment into account may account for a smaller value. However, the slower component was not observed by Shi et al., most probably because of a narrower time window and/or a different probe wavelength. On the other hand, biexponential TSSHG intensity profiles have also been detected with MG adsorbed on a silica surface.[27,44] The shortest time constant was ascribed to the decay of the S_1 state population mainly by nonradiative deactivation, whereas the other, which was much larger than that found here, was tentatively assigned to aggregates.

The smaller time constant, τ_{i1}, can be rather safely ascribed to the decay of the S_1 state population and is the equivalent of τ_{b2} found in the bulk. Its larger value compared to τ_{b2} can be assigned to the larger friction experienced at the interface, as already discussed by Eisenthal and co-workers.[25] However, the second time constant, τ_{i2}, could be in principle due to two different processes: the decay of the S_x population or the excited-state relaxation of MG aggregates. In case S_x is a vibrationally hot ground state, a slower vibrational cooling would agree with a poorer solvation of the interfacial MG molecules, hence with slower intermolecular vibrational energy transfer.[45−47] If S_x is a twisted ground-state, its relaxation to the equilibrium ground state should also depend on the local viscosity, which is apparently higher at the interface. Given the limit of error on this larger time constant, its increase by going from bulk to interface, $\tau_{i2}/\tau_{b3} = 3.3$, does not differ very much from that found with the shorter time constant, $\tau_{i1}/\tau_{b2} = 2.2$. On the other hand, the formation of aggregates at the interface might be facilitated by a higher local concentration of MG than in the bulk. The structure of MG resembles somehow that of an amphiphile molecule with a polar part, the *N*,*N*-dimethylaminophenyl groups where the

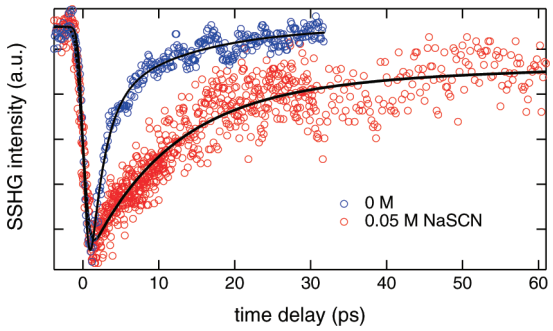

Figure 8. Intensity-normalized TSSHG profiles recorded after 615 nm excitation of MG at air/water interfaces with and without NaSCN and best biexponential fits.

positive charge is mainly localized, and an apolar part, the unsubstituted phenyl group. Thus, hydrophobic effects should favor adsorption of MG at the air/water interface. However, it should be noted that doubling the bulk MG concentration resulted in the same TSSHG profile, contrary to what would be expected if aggregates were responsible for the slow decay component.

In any case, a more precise assignment of τ_{i2} would require measurements of TSSHG profiles at different wavelengths in order to extract a decay-associated spectrum. Such broadband TSSHG is unfortunately not feasible with the setup used here.

Addition of NaCl to the aqueous phase results in a strong slowing down of the TSSHG signal as shown in Figure 7. The square root of these time profiles could also be reproduced using biexponential functions with the time constants listed in Table 2. Given the relatively low signal/noise ratio of the data measured with salt and the limited time-window, the error on the larger time constant is considerable. Moreover, the existence of an even slower decay component cannot be excluded. Thus, most τ_{i2} values in Table 2 (those with ~) should only be considered as estimates, whereas the associated amplitude, A_{i2}, can be regarded with more confidence.

Despite these uncertainties, it is immediately clear that the shorter time constant, τ_{i1}, increases continuously with the amount of NaCl, at least up to a concentration of 3 M. The larger time constant, τ_{i2}, and its amplitude, A_{i2}, increase as well but seem to saturate already at modest NaCl concentrations, i.e., around 0.3 M. Interestingly, τ_{i1} exhibits the same trend as found with the stationary SSHG intensity (Figure 6). By comparison with the TA measurements performed with 3 M NaCl (Table 1 and Figure 4), the increase of τ_{i1} can be reasonably assigned to the formation of small aggregates where the large amplitude motion of the phenyl substituents is only partially hindered. On the other hand, the larger value of τ_{i2} found with NaCl is most certainly not reflecting a slower relaxation of S_x but rather the deactivation of larger aggregates.

Whereas the presence of 0.05 M NaCl has a rather minor effect on τ_{i1}, a marked increase of this time constant is observed with NaSCN at that concentration, as illustrated in Figure 8. Here again, the square root of the TSSHG profiles have been analyzed using a biexponential function, although full signal recovery was not achieved within the time window of the measurement. Table 2 reveals that the variation of τ_{i1} with NaSCN concentration follows the same trend as that observed with the stationary SSHG intensity, namely a very strong increase already with small amounts of NaSCN and a saturation above ~0.05 M. On the other hand, the amplitude of the slower decaying component also saturates but at slightly higher concentration, i.e., between 0.05 and 0.3 M NaSCN.

As indicated in Figure 6, the strongest enhancement of the stationary SSHG intensity occurs with NaBr. Unfortunately, all measurements with this salt resulted to time profiles with too poor a signal/noise ratio for reliable time constants to be extracted.

Finally, addition of Na_2SO_4 also leads to a slowing down of the TSSHG profile. As illustrated in Table 2, the concentration dependence of the dynamics is quite similar to that found with NaCl. This agrees very well with the similar increase of the stationary SSHG intensity measured with these two salts, at least up to 0.5 M (Figure 6).

Classification of the Salts According to Their Effect on the SSHG Signal. All SSHG measurements, transient and stationary, point to a strong effect of the addition of sodium salts on the interfacial properties. Except for NaSCN, large salt concentrations ($\gg$0.3 M) have to be used to influence the excited-state dynamics of MG in bulk solution, whereas at the interface a substantial effect is already observed at moderate salt concentrations (~0.1 M). Addition of salts has already been used in several cases to enhance the SSHG intensity from air/water interfaces.[20,43,48−51] For example, in order to enhance the SHG intensity in their fourth-order Raman experiment, Fujiyoshi et al. added 0.1 M NaCl to an aqueous solution of oxazine.[51] However, our study clearly shows that the addition of salt can affect the interfacial molecular organization. Indeed, the increase of the SSHG intensity is accompanied by strong changes in the TSSHG profiles, that can be safely ascribed to the presence of aggregates. Thus, the SSHG enhancement is not just due to an increase of the interfacial concentration of solute molecules but to a change in the nature of the species responsible for the signal. MG aggregates have most probably a larger second-order nonlinear susceptibility than MG monomers. This could be due to the coherent addition of the nonlinear responses of the individual molecules in the aggregates, as expected for excitonic states. The formation of oxazine dimers at the air/water interface upon addition of NaCl has also been demonstrated by Owrutsky and co-workers.[41,52] The structure of the aggregates cannot be inferred from the present measurements. However, the change in the shape of the S_0-S_1 absorption band observed upon addition of NaCl, Na_2SO_4 and NaBr points to H-aggregates, namely aggregates where the MG molecules are in a face-to-face conformation.[30] This is also supported by their lack of fluorescence despite a longer excited-state lifetime. On the other hand, addition of NaSCN leads to aggregates of a different nature (Figure S1 in the Supporting Information) and of a much larger size given the precipitation observed at already low NaSCN concentrations.

The effect of salt on the solubility of a solute molecule in water is often discussed in terms of the Hofmeister series, where cations and anions are sorted as salting-in or salting-out agents according to their ability to enhance the solubility of albumine or to favor its precipitation and its adsorption at water surfaces.[40,53−58] Sodium is located approximately in the middle of the series for the cations. For the anions on the other hand, the Hofmeister series in order of decreasing salting-out efficiency is the following:[54]

$$H_2PO_4^- > SO_4^{2-} > S_2O_3^{2-} > F^- > Cl^- > Br^- > NO_3^- > I^- > ClO_4^- > SCN^-$$

This series has been shown to correlate rather well with the solubility of several amphiphiles.[59−61] It should be noted that it is purely empirical and that there is still no clear explanation of this effect, although it has been recently suggested that this series could be associated with dispersion forces.[20,54,62−65]

However, our results with MG can clearly not be rationalized in term of this series. Indeed, the effect of salt on the enhancement of the stationary SSHG intensity and the slowing down of the TSSHG profiles decrease in the following order:

$$SCN^- > Br^- > SO_4^{2-} > Cl^-$$

Interestingly, but for reasons that we are presently unable to explain, this observed correlation is almost the opposite of the above Hofmeister series. Indeed, according to this series, SCN^- should be a salting-in agent, whereas we observe a huge enhancement of the interfacial signal intensity at very low concentrations of this ion. One possible reason for this discrepancy could be that the Hofmeister series elaborated from the solubility of a protein in water is not universal and thus cannot simply be applied to any solute independently of its size and structure, as already suggested by several authors.[54,56,57,65] Indeed the solute−solvent interactions responsible for the solubility of a protein differ probably from those involved in the solubility of a small molecule like MG.

Concluding remarks

We have presented here a detailed investigation of the excited-state dynamics of MG in bulk and at air/water interfaces using both TA and TSSHG. Although the latter technique is very powerful for gaining a deep insight into interfacial dynamics, the interpretation of the observed data can be ambiguous and therefore a detailed knowledge of the bulk dynamics recorded under the same experimental conditions is essential. Furthermore, comparison of bulk and interfacial dynamics allows the specific properties of the interface to be evidenced. Although the excited-state dynamics of MG at air/water interfaces had already been investigated, new features have been revealed in the present study. For example, a slower recovery component of the SSHG signal that can be ascribed to the relaxation of the nonequilibrated ground-state population upon ultrafast nonradiative deactivation of the S_1 state has been observed. Furthermore, the addition of salt into the aqueous solution has been shown to not only lead to a strong enhancement of the SSHG signal intensity but also to result in a substantial slowing down of the excited-state dynamics at the interface. This investigation clearly shows that the increase of the SSHG intensity upon addition of salt is not simply due to an enhanced adsorption of the solute molecules at the interface but rather to the formation of aggregates. This should absolutely be taken into account when adding salt for enhancing the interfacial signal.

Finally, this is to our knowledge the first systematic investigation of the influence of salt at air/water interfaces using TSSHG. Although further salts need still to be explored, it appears already at this point that the conventional Hofmeister series cannot be used to predict the adsorption of a small molecule like MG at the interface.

Acknowledgment. This work was supported by the Fonds National Suisse de la Recherche Scientifique through Project Nr. 200020−115942 and by the University of Geneva.

Supporting Information Available: Absorption spectra of MG with various concentration of NaSCN. This information is available free of charge via the Internet at http://pubs.acs.org.

References and Notes

(1) Volkov, A. G. *Liquid interfaces in chemical, biological, and pharmaceutical applications*; Marcel Dekker: New York, 2001.
(2) Ishizaka, S.; Kitamura, N. *Bull. Chem. Soc. Jpn.* **2001**, *74*, 1983.
(3) Gee, M. L.; Lensun, L.; Smith, T. A.; Scholes, C. A. *Eur. Biophys. J.* **2004**, *33*, 130.
(4) Tsukahara, S.; Watarai, H. *Chem. Lett.* **1999**, 89.
(5) Brodard, P.; Vauthey, E. *Rev. Sci. Instrum.* **2003**, *74*, 725.
(6) Brodard, P.; Vauthey, E. *J. Phys. Chem. B* **2005**, *109*, 4668.
(7) De Serio, M.; Bader, A. N.; Heule, M.; Zenobi, R.; Deckert, V. *Chem. Phys. Lett.* **2003**, *380*, 47.
(8) De Serio, M.; Mohapatra, H.; Zenobi, R.; Deckert, V. *Chem. Phys. Lett.* **2006**, *417*, 452.
(9) Eisenthal, K. B. *Chem. Rev.* **1996**, *96*, 1343.
(10) Brevet, P.-F. *Surface Second Harmonic Generation*; Presses polytechniques et universitaires romandes: Lausanne, 1997.
(11) Richmond, G. L. *Chem. Rev.* **2002**, *102*, 2693.
(12) Nomoto, T.; Onishi, H. *Phys. Chem. Chem. Phys.* **2007**, *9*, 5515.
(13) Yamaguchi, S.; Tahara, T. *J. Chem. Phys.* **2008**, *129*, 101102.
(14) Tyrode, E.; Johnson, C. M.; Rutland, M. W.; Claesson, P. M. *J. Phys. Chem. C* **2007**, *111*, 11642.
(15) Ohe, C.; Arai, M.; Kamijo, H.; Adachi, M.; Miyazawa, H.; Itoh, K.; Seki, T. *J. Phys. Chem. C* **2008**, *112*, 6359.
(16) Moore, F. G.; Richmond, G. L. *Acc. Chem. Res.* **2008**, *41*, 739.
(17) Iimori, T.; Iwahashi, T.; Kanai, K.; Seki, K.; Sung, J.; Kim, D.; Hamaguchi, H.-O.; Ouchi, Y. *J. Phys. Chem. B* **2007**, *111*, 4860.
(18) Zhang, W.-K.; Wang, H.-F.; Zheng, D.-S. *Phys. Chem. Chem. Phys.* **2006**, *8*, 4041.
(19) Mitchell, S. A. *J. Chem. Phys.* **2006**, *125*, 044716/1.
(20) Petersen, P. B.; Saykally, R. J. *J. Phys. Chem. B* **2006**, *110*, 14060.
(21) Eisenthal, K. B. *J. Phys. Chem.* **1996**, *100*, 12997.
(22) Sitzmann, E. V.; Eisenthal, K. B. *J. Phys. Chem.* **1988**, *92*, 4579.
(23) McArthur, E. A.; Eisenthal, K. B. *J. Am. Chem. Soc.* **2006**, *128*, 1068.
(24) Duxbury, D. F. *Chem. Rev.* **1993**, *93*, 381.
(25) Shi, X.; Borguet, E.; Tarnovsky, A. N.; Eisenthal, K. B. *Chem. Phys.* **1996**, *205*, 167.
(26) Meech, S. R.; Yoshihara, K. *Chem. Phys. Lett.* **1990**, *174*, 423.
(27) Morgenthaler, M. J. E.; Meech, S. R. *Chem. Phys. Lett.* **1993**, *202*, 57.
(28) Duvanel, G.; Banerji, N.; Vauthey, E. *J. Phys. Chem. A* **2007**, *111*, 5361.
(29) Kemnitz, K.; Bhattacharyya, K.; Hicks, J. M.; Pinto, G. R.; Eisenthal, K. B.; Heinz, T. F. *Chem. Phys. Lett.* **1986**, *131*, 285.
(30) Czikkely, V.; Forsterling, H. D.; Kuhn, H. *Chem. Phys. Lett.* **1970**, *6*, 207.
(31) Ippen, E. P.; Shank, C. V.; Bergman, A. *Chem. Phys. Lett.* **1976**, *38*, 611.
(32) Sundström, V.; Gillbro, T.; Bergström, H. *Chem. Phys.* **1982**, *73*, 439.
(33) Mokhtari, A.; Fini, L.; Chesnoy, J. *J. Chem. Phys.* **1987**, *87*, 3429.
(34) Robl, T.; Seilmeier, T. *Chem. Phys. Lett.* **1988**, *147*, 544.
(35) Nagasawa, Y.; Ando, Y.; Okada, T. *Chem. Phys. Lett.* **1999**, *312*, 161.
(36) Miyata, R.; Kimura, Y.; Terazima, M. *Chem. Phys. Lett.* **2002**, *365*, 406.
(37) Léonard, J.; Lecong, N.; Likforman, J.-P.; Crégut, O.; Haacke, S.; Viale, P.; Leproux, P.; Couderc, V. *Opt. Express* **2007**, *15*, 16124.
(38) Yoshizawa, M.; Suzuki, K.; Kubo, A.; Saikan, S. *Chem. Phys. Lett.* **1998**, *290*, 43.
(39) Förster, T.; Hoffman, G. *Z. Phys. Chem. N.F.* **1971**, *75*, 63.
(40) Cacace, M. G.; Landau, E. M.; Ramsden, J. J. *Q. Rev. Biophys.* **1997**, *30*, 241.
(41) Steinhurst, D. A.; Owrutsky, J. C. *J. Phys. Chem. B* **2001**, *105*, 3062.
(42) Sekiguchi, K.; Yamaguchi, S.; Tahara, T. *J. Chem. Phys.* **2008**, *128*, 114715.
(43) Levinger, N. E.; Kung, K. Y.; Luther, B. M.; Willard, D. M. *Proc.SPIE* **1995**, *2547*, 400.
(44) Meech, S. R.; Yoshihara, K. *J. Phys. Chem.* **1990**, *94*, 4913.
(45) von Benten, R.; Link, O.; Abel, B.; Schwarzer, D. *J. Phys. Chem.* **2004**, *108*, 363.
(46) Kovalenko, S. A.; Schanz, R.; Hennig, H.; Ernsting, N. P. *J. Chem. Phys.* **2001**, *115*, 3256.
(47) Pigliucci, A.; Duvanel, G.; Lawson Daku, M. L.; Vauthey, E. *J. Phys. Chem. A* **2007**, *111*, 6135.
(48) Koelsch, P.; Motschemann, H. *Langmuir* **2005**, *21*, 3436.

(49) Fujiwara, K.; Wada, S.; Monjushiro, H.; Watarai, H. *Langmuir* **2006**, *22*, 2482.
(50) Bian, H.-T.; Feng, R.-R.; Xu, Y.-Y.; Guo, Y.; Wang, H.-F. *Phys. Chem. Chem. Phys.* **2008**, *10*, 4920.
(51) Fujiyoshi, S.; Ishibashi, T.-A.; Onishi, H. *J. Phys. Chem. B* **2004**, *108*, 10636.
(52) Steinhurst, D. A.; Baronavski, A. P.; Owrutsky, J. C. *J. Phys. Chem. B* **2002**, *106*, 3160.
(53) Hofmeister, F. *Arch. Exp. Pathol. Pharmakol.* **1888**, *24*, 247.
(54) Kunz, W.; Lo Nostro, P.; Ninham, B. W. *Curr. Opin. Colloid Interface Sci.* **2004**, *9*, 1.
(55) Zhang, Y.; Cremer, P. S. *Curr. Opin. Chem. Biol.* **2006**, *10*, 658.
(56) Pegram, L. M.; Record Jr, M. T. *Chem. Phys. Lett.* **2008**, *467*, 1.
(57) Lyklema, J. *Chem. Phys. Lett.* **2009**, *467*, 217.
(58) Ball, P. *Chem. Rev.* **2007**, *108*, 74.
(59) Gurau, M. C.; Lim, S. M.; Castellana, E. T.; Albertorio, F.; Kataoka, S.; Cremer, P. S. *J. Am. Chem. Soc.* **1004**, *126*, 10522.
(60) Aroti, A.; Leontidis, E.; Dubois, M.; Zemb, T.; Brezesinski, G. *Colloid and Interfaces* **2007**, *A 303*, 144.
(61) Giner, I.; Pera, G.; Lafuente, C.; Lopez, M. C.; Cea, P. *J. Colloid Interface Sci.* **2007**, *315*, 588.
(62) Kunz, W.; Belloni, L.; Bernard, O.; Ninham, B. W. *J. Phys. Chem. B* **2004**, *108*, 2398.
(63) Boström, M.; Tavares, F. W.; Finet, S.; Skouri-Panet, F.; Tardieu, A.; Ninham, B. W. *Biophys. Chem.* **2005**, *117*, 217.
(64) Garrett, B. C. *Science* **2004**, *303*, 1146.
(65) Jungwirth, P.; Tobias, D. J. *Chem. Rev.* **2006**, *106*, 1259.

JP9018662